Anomalous infra-red absorption of nanocermets in the percolation range

1998 J. Phys.: Condens. Matter 10 3679

(http://iopscience.iop.org/0953-8984/10/16/019)

J. Phys.: Condens. Matter **10** (1998) 3679–3694. Printed in the UK PII: S0953-8984(98)87589-9

Anomalous infra-red absorption of nanocermets in the percolation range

S Berthier and J Peiro

Laboratoire d'Optique des Solides, Unité associée au CNRS D0781, Université Pierre et Marie Curie, boite 80, 4 place Jussieu, 75252 Paris Cedex 05, France

Received 15 September 1997, in final form 26 November 1997

Abstract. We present a two-dimensional simulation of the optical absorption of gold granular films, using a real space renormalization procedure. This numerical effective-medium theory takes into account the actual morphology of the films. Results are compared both with experimental measurements and with other theoretical predictions asserting that the optical properties around the percolation threshold cannot be described by an effective dielectric function. Nevertheless, we obtain a good agreement between simulations and experimental data, whatever the morphology and the concentration. It is concluded on both theoretical and experimental arguments that the IR absorption can be attributed to classical surface plasmon modes, generally situated in the visible spectral range for spheroidal inclusions, broadened here towards higher wavelengths due to the formation of fractal clusters of various sizes and shapes.

1. Introduction

Scanning the purposes of the last 20 years' papers on the optical properties of inhomogeneous media, one can distinguish a major change in the approaches and field of interest. This long and thrilling period presents a threshold at the time of the publication of the *in situ* measurement made by Gadenne [1] of the optical properties of metal granular films during deposition. For the first time, the very special behaviour of composite media in the phase transition region was continuously observed and clearly exposed. The mean characteristic features are:

(1) a frequency independence of the absorptance A, reflectance R and transmittance T in the near-infrared region at the percolation threshold;
(2) a linear variation of A, R and T in the vicinity of the percolation threshold and
(3) a maximum of the optical absorption at or near the percolation threshold.

These experimental results, now widely confirmed and already observable in earlier work [2, 3], give rise to various theoretical explanations, namely the 'general aggregate theory' proposed by Robin and Souillard [4, 5] in Palaiseaux, and the scaling theory of Yagil and Deutscher [6] in Tel Aviv. These models assert the fundamental impossibility for classical effective medium theories to model the optical properties of composite materials in this concentration range, arguing that around the percolation threshold they are dominated by the fluctuations. These two approaches make an extensive use of scaling laws and percolation theory. The first assumes that only large clusters contribute to the absorption, the second that the region of strong absorption corresponds to the region where the anomalous diffusion lengths $L(\omega)$ on the backbones of the finite clusters are smaller than the correlation lengths

0953-8984/98/163679+16$19.50

ξ. In both works, the contribution of finite clusters, and therefore surface plasmon modes, qualitatively modelized by the historical theories of Maxwell Garnett [7] and Bruggeman [8], are neglected. As a matter of fact, the scaling theory and the aggregate theory are unable to modelize the plasmon absorption in the visible range, which constitutes a serious set-back. By contrast, it has been shown that all these experimental results can be understood in the framework of the effective-dielectric-function concept. Since 1986, we have proved that a renormalization process can modelize the optical properties of 2D and 3D composite media in the percolation range without any free parameters [9–11]. More recently, Brouers *et al* [12, 13] have shown that the classical mean-field theory of Bruggeman correctly modelizes the so-called anomalous absorption of granular metal observed in the infrared region. Both these effective-medium theories give a primordial role to the surface plasmon resonance absorption rather than to the fluctuations and length scale dependencies. In order to try to resolve these contradictions, we present here the results of the renormalization approach which, moreover, gives a theoretical answer to questionable assertions of other theories.

This paper is divided as follows. In a first part (section 2), we present our experimental conditions and the experimental measurements on the optical properties of granular gold films, combined with a morphological description of inhomogeneous materials which is of great interest in our approach. In section 3, the anomalous diffusion length $L(\omega)$—the relevant length scale in the scaling theory of the Tel Aviv group and the general aggregate theory of the Palaiseaux group—is briefly recalled. The well known mean-field theory of Bruggeman is then summarized with particular attention to its predictions near the percolation threshold. We then present in much more detail the real space renormalization approach. Section 4 deals with the comparison with our experimental results. Our conclusions are stated in section 5.

2. Experiments

2.1. Deposition and characterization techniques

The granular gold films are obtained by thermal evaporation onto optically polished borosilicate glass, under high vacuum (better than 10^{-8} Torr), at room temperature. The deposition rate is 0.040 ± 0.001 nm s^{-1}. During the whole deposition process, the deposited mass is measured by a quartz micro-balance which gives us, after calibration, the 'mass thickness', i.e. the thickness that would have a continuous film of the same weight. The film resistance is also continuously measured between two parallel gold strips 3 cm apart. This allows us to precisely determine the critical mass thickness d_c at which the electrical percolation threshold occurs. Following a classical technique [14, 15], the morphology of the films can be modified by heat treatment. Just after deposition, half of the films are annealed under vacuum at 98 °C for 24 hours. This deeply affects their geometrical, optical and electrical properties. The comparison of the properties of the films obtained by these two growth processes constitutes an important point in this work.

The optical properties are determined *ex situ* on a Varian Cary 5 spectrometer, in the range 0.35–3 μm, by measuring the absolute reflectance R and transmittance T under normal incidence. The absorptance of the films $A = 1 - R - T$ is then calculated. After completion of all electrical and optical measurements, the samples are covered by a thin graphite layer and removed from the substrates by a chemical method. They are then observed by transmission electron microscopy (TEM). TEM micrographs are scanned and digitized on 512×512 pixels at 256 grey levels. Special attention is given to the determination of the nature of the pixels (metallic or insulating), in order to take care of the tiny connections

between clusters near the percolation threshold (called red sites in percolation terminology). An image processing has been developed leading to an unambiguous optimum binarization threshold [16]. The most sensitive test, after comparison of the experimental and calculated metal concentration, consists in verifying the connectivity of an infinite cluster throughout the image.

The surface coverage parameter p of each sample is determined in the image. The results are compared to the average mass thickness d and show a linear relation (figure 1). It is worth noticing that (except at the percolation threshold p_c) the reduced values $(d - d_c)/d_c$ and $(p - p_c)/p_c$ are always different. We also calculated the cluster and the hole size distributions and their mean size. The fractal dimension of the infinite cluster (above percolation) or the mean fractal dimension of the largest clusters (below percolation) are then determined by two different methods. For $p < p_c$, the clusters have slightly different fractal dimension and only a mean value can be determined by plotting the logarithm of the perimeter P versus the surface S of the clusters. The slope of the linear part of this curve gives the mean fractal dimension using the relation $P \propto S^{Df/2}$. For $p \geqslant p_c$, the infinite cluster is isolated and we determine the mean fraction $M(L)$ of pixels belonging to it and contained in a square box of variable size L, related to the fractal dimension by

$$M(L)/L^2 \propto L^{Df-2}. \tag{1}$$

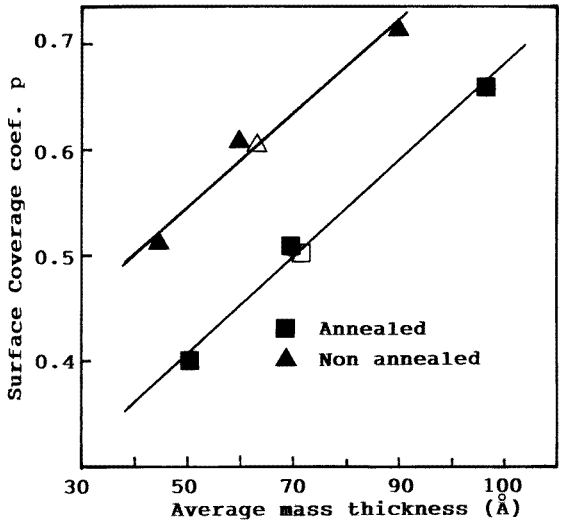

Figure 1. Relation between the surface coverage parameter p as determined by image treatment and the average mass thickness for the annealed ■ and non-annealed ▲ films. White symbols □ and △ denote the percolation values.

2.2. Results

Figure 2 shows the TEM micrographs of three samples, annealed and non-annealed. One can easily see that sample A is below the percolation threshold p_c, sample B is very close to p_c and sample C well above it, whatever the thermal treatment. This is confirmed by the optical analyses and the dc measurements. For the annealed samples, $p_c = 0.50$ and we have respectively $p(\mathrm{A}) = 0.4$, $p(\mathrm{B}) = 0.52$, $p(\mathrm{C}) = 0.67$. For the non-annealed,

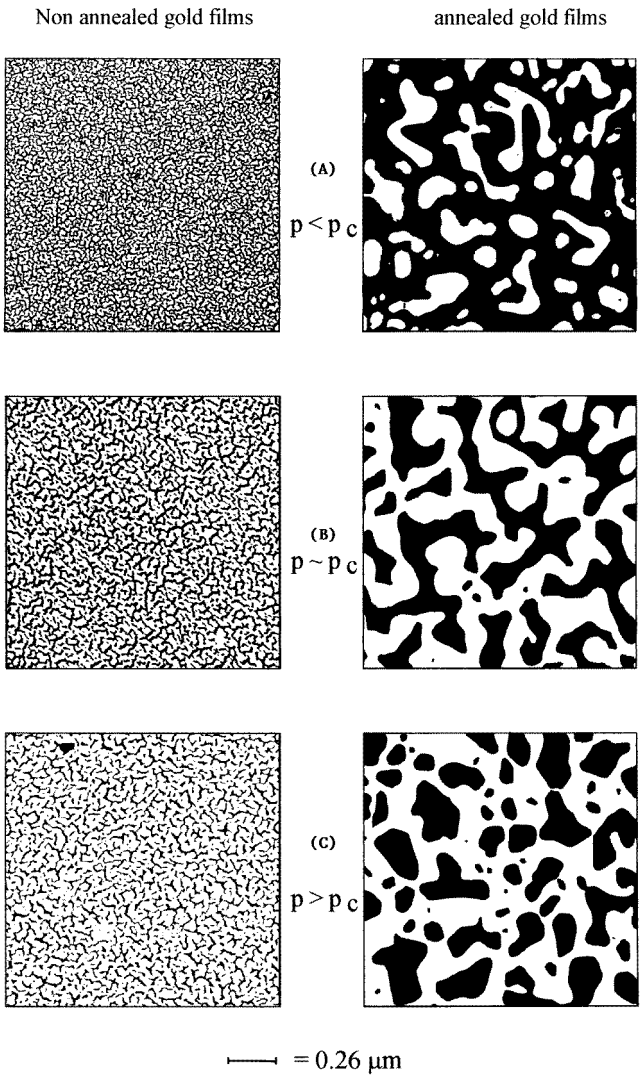

Figure 2. Digitized TEM micrographs of the two sample sets of gold granular films: as deposited on the left; after 24 hours annealing at 98 °C on the right. Metal is in white.

$p_c = 0.62$ and the concentrations are $p(\mathrm{A}) = 0.52$, $p(\mathrm{B}) = 0.63$, $p(\mathrm{C}) = 0.72$. Other important morphological results are listed in table 1.

As expected, the annealed films are always constituted by fewer but larger clusters than the non-annealed ones: the basic scales of the correlation length ξ_0 for these two samples sets are approximately $\xi_0 \sim 25$ nm for non-annealed films and 150 nm for annealed ones. (ξ_0 is the prefactor of the percolation scaling law: $\xi = \xi_0(p - p_c)^{-\nu}$ and corresponds to the size of the elementary constituent of the inhomogeneous medium i.e. approximately the average width of the arms of the fractal clusters.) As a consequence of the thermal mobility, the fractal dimension is always lower in the case of annealed films. At least, the critical thresholds d_c and p_c follow the linear variation of d and p.

Table 1. Mean geometrical and electrical charcteristics of the samples.

	d (Å)	$d^* = (d - d_c)/d_c$	p	$p^* = (p - p_c)/p_c$	D_f	$R\square$ (Ω)
Annealed A	50.7	−0.26	0.4	−0.4	1.8	∞
Annealed B	69.9	0.013	0.52	0.04	1.83	194
Annealed C	107.4	0.56	0.67	0.34	1.88	7.2
Non-ann. A	44.8	−0.24	0.52	−0.16	1.98	∞
Non-ann. B	60.1	0.019	0.63	0.016	1.90	231
Non-ann. C	90.4	0.53	0.72	0.16	1.93	11

Another interesting point is the relative dependence of the gold grain morphology and the hole morphology with the deposition process. In the case of annealed films, holes and metallic phase have the same behaviour. In the case of non-annealed films, the metallic phase is more dense than the insulating one, and the morphology is not symmetric.

2.3. Optical measurements

The reflectance R and transmittance T of the samples presented above are shown in figure 3(a, b).

Below the percolation threshold, both annealed and non-annealed films are clearly insulator-like. The reflectance, decreasing with wavelength, is relatively low. It is lower in the case of annealed film than in the case of non-annealed ones. Above p_c, the films show a clear metallic behaviour (high reflectance and low transmittance at long wavelength). Reflectance and transmittance of annealed and non-annealed films differ in such a way that the absorptance remain constant versus wavelength. Near the percolation threshold, as already shown by Gadenne *et al* in [1], the optical behaviours of the films are nearly independent of the wavelength in the infrared region. At the same time, the optical properties of annealed and non-annealed films are similar and thus independent of their morphology.

Finally, the stability of R, T and A below $\lambda \approx 0.55$ μm may be noticed. It is due to the occurrence of gold inter-band transitions which dominate the optical behaviours in this region.

From these different results, it becomes clear that the optical properties of granular materials are affected by morphological fluctuations except in the vicinity of the percolation threshold. Many attempts have been made to quantify the individual influence of a few morphological and structural parameters [17, 18] like volume concentration p, fractal dimension of the largest and infinite clusters, size distribution.... The conclusions are (1) these parameters are highly correlated and (2) they affect the percolation threshold value, and therefore the reduced concentration $(p - p_c)$. At given values of the wavelength ($\lambda = 1.7$ μm and $\lambda = 2.2$ μm, corresponding to the experimental data given by Gadenne) we have compared all our experimental results, taking $(p - p_c)$ as the main parameter. Figure 4 shows that at and around the percolation threshold, R, T and A of annealed and non-annealed films are close to each other, whatever the morphology. Close to the percolation and over a wide concentration range around it, a large optical absorption—the so-called IR anomalous absorption—is found. It weakly depends on the optical frequency. As already pointed out, the absorptance is maximum for a filling factor slightly higher than the percolation threshold. This will be discussed later, after than the competitive models have been presented.

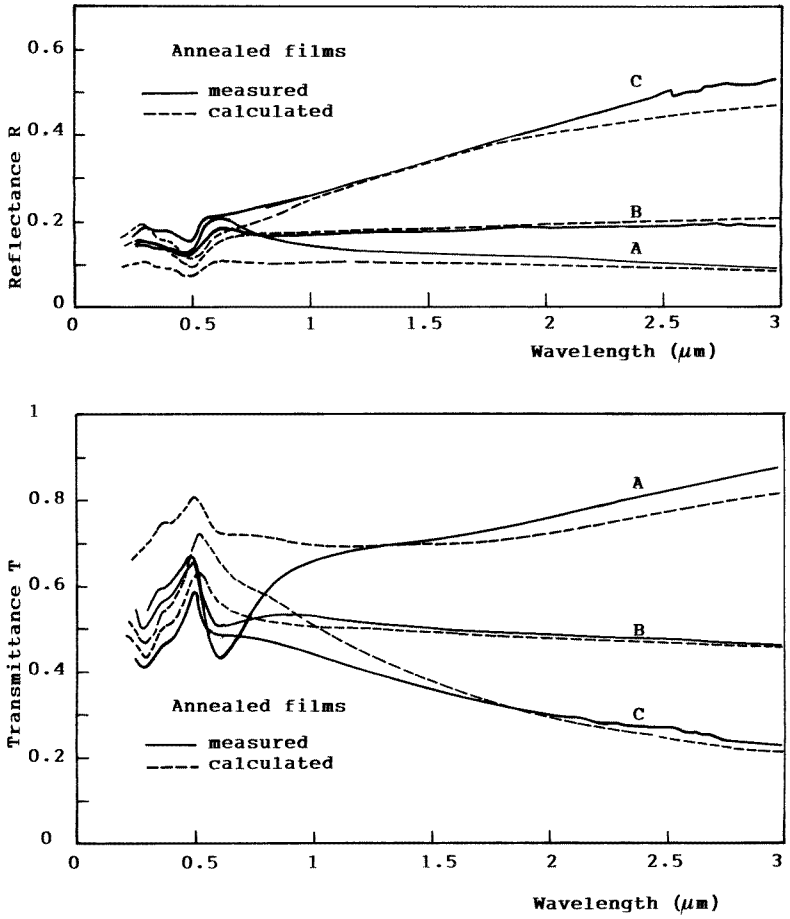

(a)

Figure 3. Reflectance R and transmittance T of the two sample sets (——) versus wavelength in the visible and near infra-red. Comparison with the renormalization process predictions (– – –).

3. Theories

3.1. The scaling based models

These models are based on the assumption that the effective dielectric function has no physical meaning close to the percolation threshold. The optical properties can only be defined by averaging on different areas of size L where the films have different properties.

In the model proposed by the Tel Aviv group [6], these areas are on the size of the anomalous diffusion length which depends of the optical frequency $L(\omega)$ if $L(\omega) \ll \xi$ and $L = \xi$ at the opposite limit. On a percolation lattice, $L(\omega)$ is related to the classical critical exponents by

$$L(\omega) = L_0(1/k\xi_0)^{1/2+\theta} \tag{2}$$

where k is the wavenumber and L_0 a coefficient of the order of unity. $\theta \sim 0.8$ for 2D systems and ξ_0 is the basic scale of the percolation correlation length

$$\xi = \xi_0(p - p_c)^{-\nu} \tag{3}$$

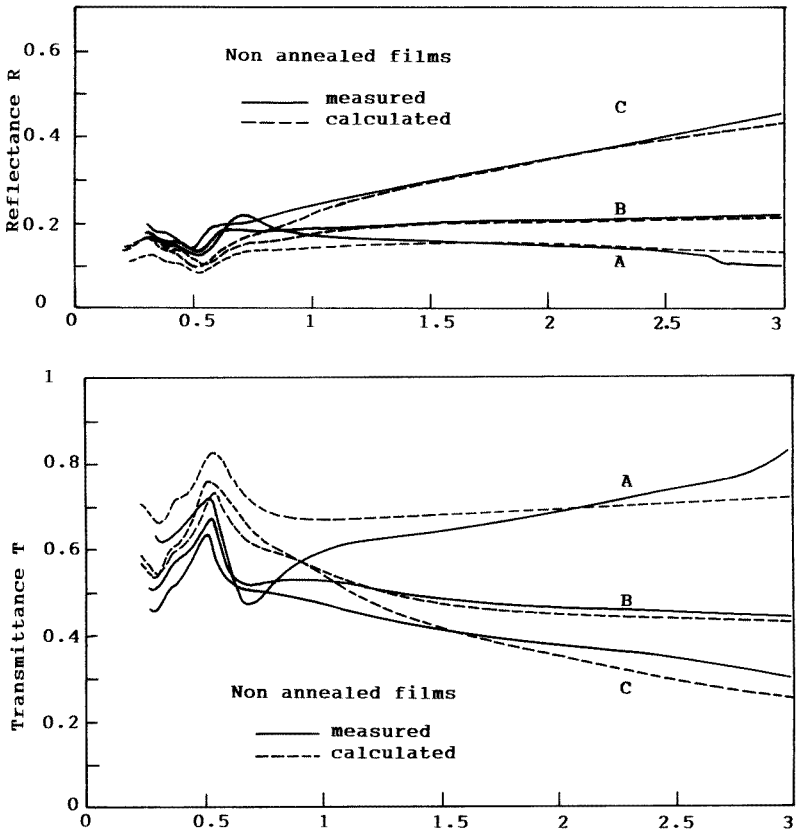

(b)

Figure 3. (Continued)

with $\nu = 4/3$. The parameters retained by Yagil *et al* for the scaling are $L_0 = 4$ and $\xi_0 = 10$ nm. Notice that $L(\omega)$ is independent of the concentration p for a percolation lattice (random distribution) and nearly independent of ω for small values of ξ_0. On the other hand, ξ only depends on the concentration p. Figure 5 shows this variation, together with the absolute value of $L(\omega)$ for $\lambda = 2.2$ μm. In this example, the electronic diffusion length is limited by the geometric correlation length for most the concentrations, except in a small concentration range in the vicinity of the percolation threshold, much smaller than the anomalous absorption range. The frontier between the two regimes is governed both by ξ_0—which can be experimentally determined—and L_0 which is a free parameter.

The approach of the general aggregate theory [4] is somewhat different but uses a similar length scale δ. Its aim is to determine the electromagnetic response of a single aggregate. The result is then extended to the macroscopic properties of the composite. The authors write a differential equation for the average current density $j(x)$ in the fractal aggregate, called the 'general antenna equation' incorporating the main physical effects in the aggregate via R, L, C values. This equation is then solved in the WKB approximation framework, for a source located at the origin. It can be shown that a length δ exists, above which the current is no longer correlated with the origin: this current correlation length can be simply related to the anomalous diffusion length $L(\omega)$ of the previous model for percolation fractal

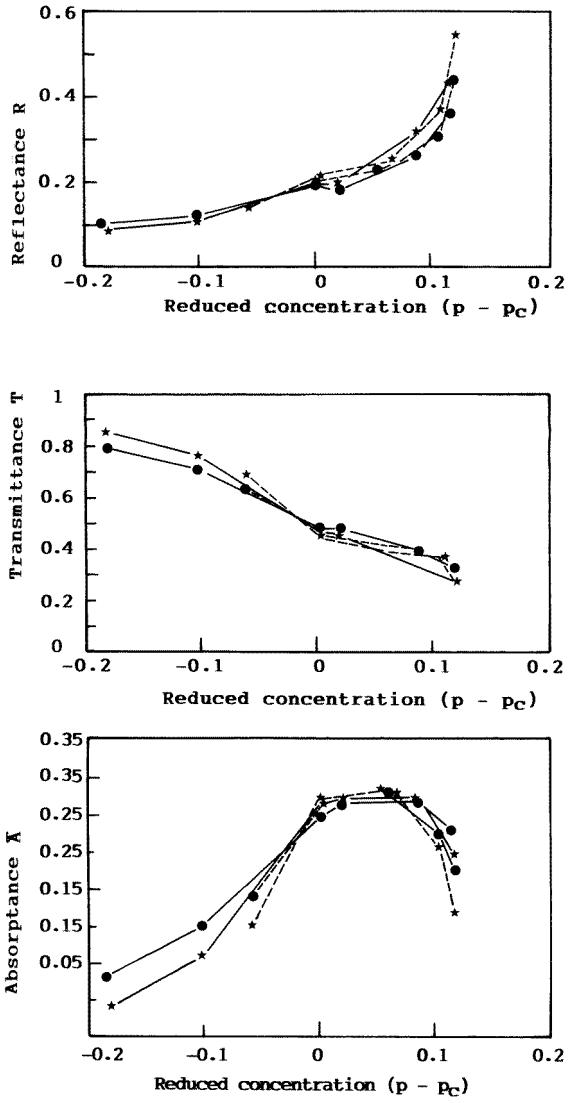

Figure 4. Plots of the experimental reflectance R, transmittance T and absorptance A of the annealed (——) and non-annealed (– – –) films versus the reduced concentration $(p - p_c)$ for two IR wavelengths ($\lambda = 1.7$ μm ● and $\lambda = 2.2$ μm ★). Near the percolation threshold ($p^* = 0$), the optical behaviour is nearly independent of the wavelength.

aggregates. The aggregate is then considered as a set of blocks of size δ, and its properties are obtained by summing over all blocks, in the same way as the previous model.

The common features of these models are (i) to determine a characteristic scale of observation of the inhomogeneous medium, (ii) to calculate (by different approaches) the optical response of blocks of this size, (iii) to average these optical responses over the different blocks. Both these models give a good account of the optical properties of the medium in the IR range; they cannot be accepted in this form, for they neglect the plasmon absorption, observed since one century, which can also explain, as shown by Brouers *et al*

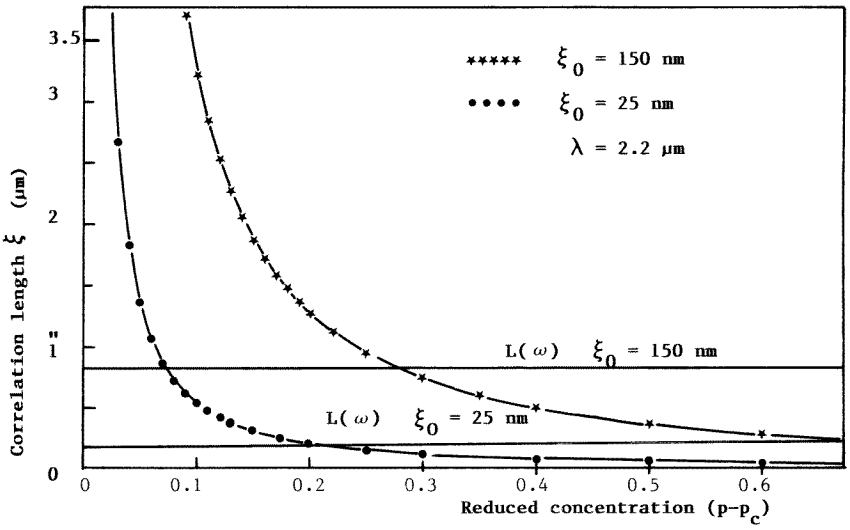

Figure 5. The correlation length ξ versus the reduced concentration $(p - p_c)$ (the prefactor ξ_0 values are $\xi_0 = 25$ nm for the non-annealed films (●●●) and $\xi_0 = 150$ nm for the annealed ones (★★★)).

[12], or ourselves, the anomalous IR absorption. Other important restrictions for these models is (1) that they are concerned with pure random media, governed by the percolation theory, which is not the case for real granular media and (2) that they deny any role to the plasmon modes in the IR range by neglecting the finite clusters smaller than $L(\omega)$.

We will now show that a real space renormalization approach avoids these two restrictions, first by taking into account the real morphology of the inhomogeneous medium, second by incorporating the effect of each aggregate, whatever its size.

3.2. Effective-medium approaches

3.2.1. The Bruggeman theory. The definition of an effective medium assumes the definition of an average electric field or an average current. In the mean-field theory proposed by Bruggeman in 1935, each component is embedded in the effective medium and the average field is the spatial average of the fields inside the various components, leading to the expression of an effective dielectric function ε_e:

$$\sum_k p_k(\varepsilon_k - \varepsilon_e)/[\varepsilon_e + A_k(\varepsilon_k - \varepsilon_e)] = 0 \tag{4}$$

where p_k is the relative volumic concentration and A_k the depolarization factor of the ellipsoidal inclusion of component k. It has been known for a long time that the Bruggeman theory predicts a percolation transition for a critical concentration $p_c = A$. For a two-component metal (ε_m)–dielectric (ε_i) mixture with the same depolarization factor A, this equation reduces to

$$p(\varepsilon_a - \varepsilon_e)/[\varepsilon_e + A(\varepsilon_a - \varepsilon_e)] + (1 - p)(\varepsilon_b - \varepsilon_e)/[\varepsilon_e + A(\varepsilon_b - \varepsilon_e)] = 0. \tag{5}$$

The physical solutions of this second-order complex equation are generally difficult to establish, except in the purely symmetric situation where $A = p_c = 1/2$. One can

notice however that this particular case corresponds to the Bruggeman approximation for 2D composites. We will show that general interesting considerations on the behaviour at and near percolation can be easily drawn in this particular case. Equation (5) reduces to:

$$\varepsilon_e^2 - 2\varepsilon_e[(\varepsilon_a - \varepsilon_b)(p - 1/2)] - \varepsilon_a\varepsilon_b = 0. \tag{6}$$

For the critical concentration $p = p_c = 1/2$, one has:

$$\varepsilon_e^2 = \varepsilon_i\varepsilon_m \tag{7}$$

where the indices i and m now refer to the insulating and metallic components respectively. For a quantitative analysis ε_i is assumed to be real and independent of wavelength, and ε_m is assumed to be given by the Drude formula for free electrons:

$$\varepsilon_m(\omega) = P - \omega_p^2/\omega(\omega + \mathrm{i}/\tau) = \tilde{n}^2 = (n + \mathrm{i}k)^2. \tag{8}$$

In the near-IR range considered here ($\omega_\tau \ll \omega \ll \omega_p$), the real and imaginary part of $\varepsilon_m(\omega)$ take the asymptotic forms:

$$\begin{cases} \varepsilon_1 = n^2 - k^2 \approx P - \omega_p^2/\omega^2 \\ \varepsilon_2 = 2nk \approx \omega_p^2\omega_\tau/\omega^3 \end{cases} \tag{9}$$

so that:

$$\begin{cases} n \approx \omega_p/2\omega^2\tau \\ k \approx \omega_p/\omega. \end{cases} \tag{10}$$

At percolation, the effective dielectric function predicted by the Bruggeman theory is then:

$$\varepsilon_e = \sqrt{\varepsilon_i\varepsilon_m} = \sqrt{\varepsilon_i}\tilde{n} = \sqrt{\varepsilon_i}[\omega_p/2\omega^2\tau + \mathrm{i}\omega_p/\omega] \tag{11}$$

and the effective optical absorption at percolation

$$\varepsilon_{2e}/\lambda = \sqrt{\varepsilon_0\varepsilon_i}/\lambda_p. \tag{12}$$

The optical absorption at p_c is independent of the wavelength but depends on both the inclusion and the matrix materials. The plasma frequency of metallic grains ω_p is relatively independent of the morphology of the grains (beyond the size of the quantum size effects). However the effective value to be used for ε_i must take into account the image charge effect, and therefore depends on the substrate nature. Various values have been used by different authors ranging from 1 (dielectric constant of vacuum) up to ε_s (dielectric function of the substrate). In 1983, Bedeaux and Vlieger [19–21] calculated the optical thickness of discontinuous gold film by using the polarizability density autocorrelation function. They have established that

$$\varepsilon_i = (1 + \varepsilon_s)/2 \tag{13}$$

is the proper choice to calculate the susceptibility of islands. According to equation (12), the value of ε_i clearly has a strong influence on the absorption of the films. The optimum value given in section 4.2 is in very good agreement with this theoretical prediction.

3.2.2. The renormalization approach. In order to take into account the actual morphology of the inhomogeneous medium, we have developed since 1987 effective-medium models based on 2D and 3D position space renormalization [9, 10]. In order to compare with other approaches, only the 2D renormalization will be presented here. The first aim of this approach is to take into account all the intrinsic morphological parameters, by applying a phenomenological theory to real TEM images. It was remarkably perceptive of Bedeaux and Vlieger [19] in 1973 to introduce this concept. In their theory, the average polarizability

of the islands is determined via the actual density autocorrelation function, evaluated on an electron micrograph. It constitutes, to our knowledge, the first direct treatment of a real morphology. Our approach is somewhat different but, like theirs, does not lead to any mathematical expressions. The advantage of these numerical models is that they can be associated with different image treatments or growth simulations for prospective investigations.

The principle of the renormalization approach in real space [22–24], as first introduced by Kadanoff [25], for magnetic materials, assumes that one can discuss blocks of inclusions as if they were single inclusions whose properties, changing from one block to the other to account for local morphological parameters, are determined by classical effective-medium theory. Iteration of this procedure allows successive reductions of the number of effective inclusions, until, finally, one reaches a unique block with effective optical properties of the whole average medium. The process is the following. (i) The initial lattice (size L) (digitized electro-micrograph or computer simulated lattice) is divided into blocks of four sites characterized by their respective dielectric function (DF) (generally $\varepsilon_d \approx$ constant, for the dielectric, $\varepsilon_m(\omega) = P - \omega_p^2/(\omega + \mathrm{i}/\tau)$ for the free electron metal). (ii) Blocks are then reduced to local unit cells whose effective DF is determined using a classical effective-medium theory (here Maxwell Garnett theory modified by Cohen *et al* [2])

$$\varepsilon_e = \varepsilon_d \frac{\varepsilon_m[A + p(1-A)] + \varepsilon_d(1-p)(1-A)}{\varepsilon_m A(1-p) + \varepsilon_d[1 - A(1-p)]}. \tag{14}$$

A conduction criterion is adopted to decide which component will be considered as a matrix and which one as an inclusion: the matrix in the unit cell (DF ε^{ma}) is the average component through which one can go from one side of the block to the other one, following the field direction. (iii) Following Kadanoff's method, the new lattice (size $L/2$) is divided one more time into blocks and the process is repeated until $L = 1$. This transformation, usually denoted R_2, allows us to pass from a description of the film at length scale a (size of the initial pixel) to a description of the same system at length scale $2a$. When the whole process is repeated until the last block gives the average properties of the initial lattice, this has been analysed at any length scale, from the initial pixel—which should be smaller than ξ_0—up to the entire lattice which must be larger than ξ. It is thus obvious that at a given intermediate step the lattice has been analysed at a length scale close to $L(\omega)$. This point and the evolution after this step will be discussed later.

This approach has been presented in detail in previous papers [9, 10], and was shown to be able to give a good account of the percolation transition at p_c, without any free parameters, both in 2D and 3D cases. We want now to focus our attention on the modelization of the optical properties of percolating films and show that this effective-medium theory is experimentally justified, both qualitatively and quantitatively.

3.2.3. Theoretical predictions. It is first worth noticing that the critical concentration p_c is known to be a non-trivial fixed point in the renormalization process. The concentration of a lattice exactly at percolation is an invariant for the renormalization transformation. As a consequence, the process is very slowly converging for small reduced concentrations p^* (i.e. concentrations p close to p_c) and large initial lattices need to be used.

The calculated reflectance R and transmittance T of the granular Au films, including the substrate contribution, are shown in figure 3. They have been calculated using Abeles thin-film formulae [26], with the dielectric function of the films derived from the renormalization process as applied to the image. The film thicknesses used in these formulae are the effective thicknesses obtained by dividing the experimental mass thicknesses measured during the

evaporation process by the concentration p. The model gives a good account of the experimental results both in the visible and in the IR ranges, especially near the percolation threshold (films B) where EMTs are supposed to fail. The frequency independence of the optical properties in the IR range at percolation is also accurately reproduced.

The most important result concerns films (B) which are close to the percolation threshold. The correlation lengths in these films are larger than $L(\omega)$ but still lower than the initial lattice size, so that the average properties are reached before the end of the renormalization process. This can be seen in figure 6, where the trajectories of the renormalized reduced concentrations are plotted for different initial concentrations, as a function of the number of renormalization steps, i.e. the size of the analysed block. Annealed films are on the right-hand side, non-annealed ones on the left.

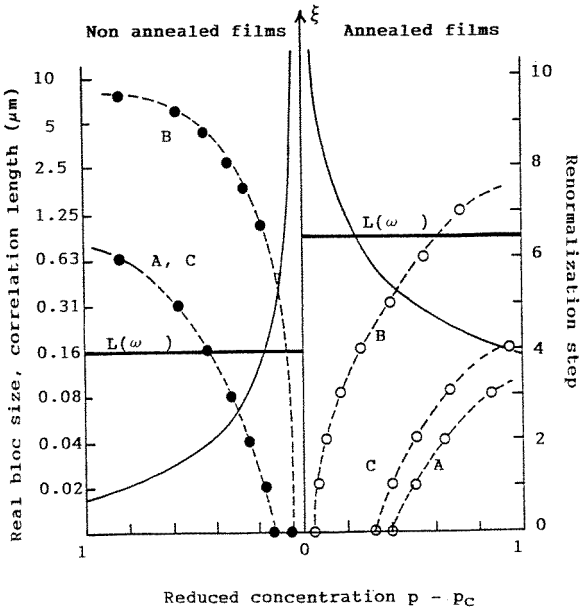

Figure 6. Evaluation of the renormalized reduced concentration with the number of renormalization steps (N) or the initial lattice size expressed in pixels or in real size (1 pixel $\equiv$ 98 Å in our examples). Annealed films are on the right. For non-percolated films (i.e. negative reduced concentrations) the absolute value $|p - p_c|$ is plotted. For the two sample sets, we also plot the correlation length versus the reduced concentration and the anomalous diffusion length $L(\omega)$ for $\lambda = 2.2$ μm.

This figure allows a quantitative comparison of the different length scales $L(\omega)$ ($\lambda = 2.2$ μm) and ξ. ξ_0 is of the order of 25 nm for non-annealed films and 150 nm for annealed ones. Different forms and absolute values of ξ and $L(\omega)$ are therefore obtained for the two sets of films.

Three important observations arise from these comparisons. (i) Whatever the film, the analysed sample is always larger than the correlation length. From a static point of view, the samples are representative of the films. (ii) For all the films considered here, the renormalized reduced concentrations always tends toward 1 (or -1 for non-percolated films) before the process stops. Further iterations slightly affect the absolute values of the effective

DF and are strictly equivalent to an averaging of the different blocks. (iii) Except for very small reduced concentrations (samples B), $L(\omega)$ is larger than ξ so that the frequency effects are negligible and the quasi-static approximation can be used.

The concentration range where the renormalization process cannot be successfully applied therefore appears to be very small. It corresponds to reduced concentrations $|p^*| < 4 \times 10^{-2}$, whereas the range of observation of the anomalous absorption is much larger: $|p^*| < 0.4$.

4. The anomalous IR absorption

4.1. Relevant parameters

Particular attention is now given to this so-called anomalous absorption. First of all, we want to focus attention on the different parameters used for its characterization, which can be at the root of much confusion. For 2D and 3D systems, the absorption coefficient and the absorptance can be plotted versus the metal concentration p (and the associated reduced concentrations $p - p_c$, $(p - p_c)/p_c, \ldots$), while for 2D systems, as considered here, films can also be characterized by the mass thickness d (and the reduced mass thicknesses $d - d_c$, $(d - d_c)/d_c, \ldots$). It is worth noticing that these two bases are not equivalent. d and d_c are generally determined using calibrated quartz micro-balances and d_c measurements, while p and p_c (for 2D systems) are deduced from image treatment. A linear relation between p and d is generally assumed and is confirmed here. This relation holds for $(p - p_c)$ and $(d - d_c)$ or $(p - p_c)/p_c$ and $(d - d_c)/d_c$. From a theoretical point of view however, the pure symmetric reduced scale should be $p^* = (p - p_c)/p_c$ for $p < p_c$ and $(p - p_c)/(1 - p_c)$ for $p > p_c$ so that $p^* = \pm 1$ when $p = \{0, 1\}$. A similar scale for d^* should introduce the mass thickness corresponding to the continuous film as an upper limit for d, equivalent to the concentration $p = 1$. From the point of view of percolation, these different scales only affect the prefactor of the power laws. These distinctions are rarely made. They may lead to significant discrepancies far from the percolation threshold. Although we are not concerned here with 3D experiments, it is worth noticing that these remarks are not relevant in this case. In contrast to the 2D case where the concentration p and the mass thickness are proportional, p and d are independent in the 3D case. As a matter of fact, the absorption A depends on these two parameters. ε_2 (or ε_2/λ) which only depends on p is then the only relevant parameter for 3D experiments.

The absorption itself is much more questionable. The physical quantity which is directly derived from the optical measurements R (reflectance) and T (transmittance) is the absorptance $A = 1 - R - T$. R and T are corrected from internal multiple reflections in the substrate. Most experimental papers represent A versus d (or $d - d_c$). On the other hand, the theoretical approaches calculate an effective dielectric function $\varepsilon = \varepsilon_1 + \mathrm{i}\varepsilon_2$ (or the effective complex conductivity σ) from which the optical absorption coefficient $\alpha = 4\pi k/\lambda$, where k is the imaginary part of $\sqrt{\varepsilon}$, is calculated. Most authors however give ε_2/λ (or $2\pi\varepsilon_2/\lambda$), also called optical absorption coefficient) but it is worth noticing that generally these quantities are not proportional.

Optical properties of homogeneous films of thickness e deposited on a non-absorbing substrate (real optical index n_s) can be calculated by the matrix technique established by Abeles [26]. When the film thickness e is much smaller than the wavelength, second-order development in e/λ gives a linear relation between ε_2/λ and A/T:

$$\frac{A}{T} \approx 2\pi \frac{\varepsilon_2}{\lambda} \frac{e}{n_S}. \tag{15}$$

Moreover, whatever the approach, either for the determination of ε from experimental R and T measurements, or for the calculation of R and T from theoretical ε values, a thickness has to be defined which is not the mass thickness and acts as a free parameter.

4.2. Comparisons

Figure 7 shows the IR optical absorption ε_2/λ as calculated with the renormalization theory for $\lambda = 2.2$ μm, to allow comparison with other experimental data and predictions of other models. As experimentally observed, the optical absorption is maximum for a concentration slightly higher than p_c. As we shall argue, the renormalization theory is in good agreement with the experimental results, both for the amplitude and the width of the absorption peak.

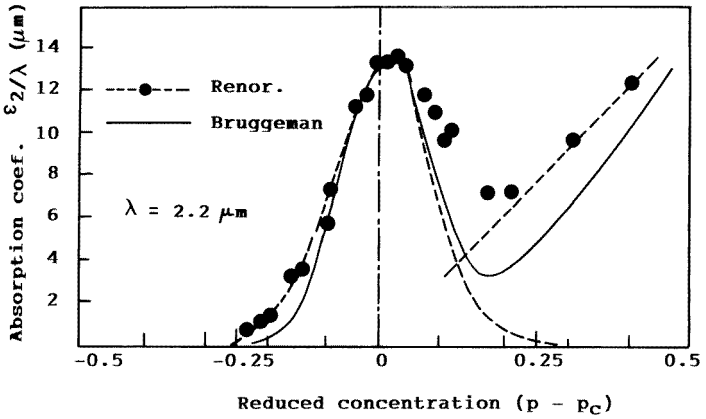

Figure 7. Optical absorption ε_2/λ of simulated gold granular films versus the reduced concentration $(p - p_c)$ deduced from the renormalization (●) and the Bruggeman theory (——). In the former, absorption from plasmons in the finite clusters and by conduction in the infinite cluster have been distinguished (– – –).

The optical absorption coefficient ε_{2e}/λ is of the order of 13 μm^{-1} at percolation for the two sets of films, whatever the wavelength. This value is correctly predicted by the Bruggeman theory for gold particles ($\hbar\omega_p \sim 10$ eV) deposited on a dielectric substrate $\varepsilon_s \sim 2.8$. Equations (14) and (15) give $\varepsilon_{2e}/\lambda = 11.2$ μm^{-1}. It is possible to reproduce the experimental value by assuming a higher value of ε_i, closer to ε_s.

According to the local calculation at each renormalization step (i.e. Maxwell Garnett theory), the absorption is attributed to plasmon modes in the finite clusters. In spherical inclusions, these modes are generally situated in the visible spectra and moved toward higher wavelengths when the concentration rises. Near percolation where all the cluster sizes exist, all the modes are taken into account by the renormalization process, leading to the large absorption peak around p_c. Above p_c, the absorption by the electrons of conduction in the infinite cluster is superimposed so that the maximum is slightly moved toward high concentrations. This contribution can be described using a Drude function (as presented in [9] and [10]) and subtracted from the total absorption. The plasmon absorption peak is then centred at the percolation threshold (figure 7).

We want now to focus our attention on these results. Figure 8(a, b) shows the experimental absorpance $A = 1 - R - T$ for the annealed and non-annealed gold films as a function of the concentration p (figure 8(a)) and of the reduced concentration p^*

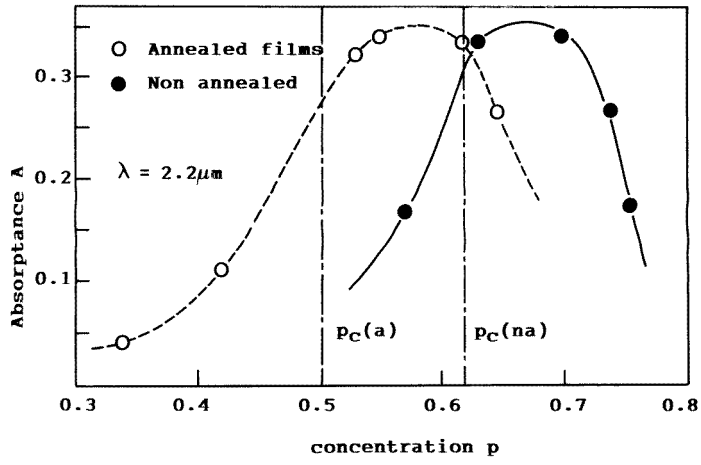

(a)

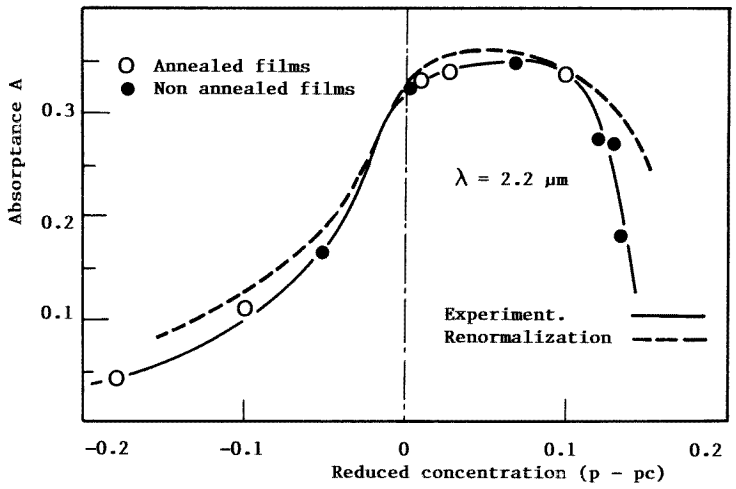

(b)

Figure 8. Experimental absorptance of the annealed (○) and non-annealed (●) films for $\lambda = 2.2\ \mu$m as a function of the concentration p (a) and of the reduced concentration $p^* = p - p_c$ (b). Comparison with the experimental results (——) (b).

(figure 8(b)). Despite very different morphologies, the absorption near the percolation threshold appears to be similar for the two sets of films, and so independent of the morphology. As a consequence, this allows us to calculate the optical properties of an inhomogeneous medium on random lattices, easily generated by small computers. It also validates the scaling approaches presented before that only used the numerical results of the percolation theory on pure random lattices rather than real structures.

The absorptance $A = 1 - R - T$ of the two sets of films versus the reduced concentration is shown in figure 8(b) for $\lambda = 2.2\ \mu$m, together with the theoretical predictions. Over a wide range of concentrations, the renormalization theory provides a good description of the so-called anomalous absorption. Particularly noteworthy is the fact that these results are obtained from real TEM micrographs without any free parameters. The fit can be improved by modifying the effective thickness, i.e. making hypotheses on the shape of the inclusions.

5. Conclusion

The optical properties of two sets of gold discontinuous films, presenting very different morphologies and percolation parameters, have been determined and analysed in the mean-field concept framework.

Many remarks arise from this work. (i) Despite very different morphologies and percolation threshold values, the absorption is similar for the two sets of films, when plotted versus the reduced quantities $p^* = p - p_c$ or $d^* = d - d_c$. (ii) Over a wide range of concentrations, the renormalization theory provides a good description of the so-called anomalous absorption. The frequency independence and the maximum of the optical absorption in the percolation range are correctly predicted. According to the local calculation performed at each step of the renormalization process, the absorption is attributed, after subtracting the conduction contribution above p_c, to the plasmon modes parallel to the surface in the fractal clusters. (iii) Effective-medium theories, when related to the actual morphology of the medium, can account for the special behaviour of granular films in the IR range, at and near the percolation threshold. Furthermore, the classical mean-field theory of Bruggeman predicts the IR absorption and gives prominence to the substrate nature. For gold granular films, the absorption amplitude is quantitatively reproduced for an inter-island dielectric constant close to that of the substrate.

Nevertheless, the assertion that the optical properties of inhomogeneous media near the percolation threshold cannot be described by an effective dielectric function collapses.

References

[1] Gadenne P, Yagil Y and Deutsher G 1989 *J. Appl. Phys.* **66** 3019
[2] Cohen R W, Cody G D, Couts M T and Abeles B 1973 *Phys. Rev.* B **8** 3689
[3] Bedeaux D and Vlieger J 1974 *Physica* **73** 287
[4] Robin T and Souillard B 1989 *Opt. Commun.* **71** 15
[5] Robin T and Souillard B 1993 *Physica* A **193** 79
[6] Yagil Y, Josephin M, Bergman D J, Deutsher G and Gadenne P 1991 *Phys. Rev.* B **43** 11 342
[7] Maxwell Garnett J C 1904 *Phil. Trans. R. Soc.* **203** 383
[8] Bruggeman D A 1935 *Ann. Phys., Lpz.* **24** 636
[9] Berthier S, Driss-Khodja K and Lafait J 1987 *Europhys. Lett.* **4** 1415
[10] Berthier S and Driss-Khodja K 1989 *Opt. Commun.* **70** 29
[11] Depardieu G, Fiorini P and Berthier S 1994 *Physica* A **207** 110
[12] Brouers F, Clerc J P and Giraud G 1991 *Phys. Rev.* B **44** 5239
[13] Brouers F, Clerc J P, Giraud G, Laugier J M and Randriamantany Z A 1993 *Phys. Rev.* B **47** 666
[14] Jarret D N and Ward L 1976 *J. Phys. D: Appl. Phys.* **9** 1515
[15] McKenna W T and Ward L 1981 *Phys. Status Solidi* a **68** K11
[16] Beghdadi A, Constans A, Gadenne P and Lafait J 1989 *Revue Phys. Appl.* **21** 73
[17] Peiro J, Berthier S and Driss-Khodja K 1993 *Nanostruct. Mater.* **2** 421
[18] Peiro J 1994 *Thesis* Université Pierre et Marie Curie, Paris
[19] Bedeaux D and Vlieger J 1973 *Physica* **67** 55
[20] Bedeaux D and Vlieger J 1976 *Physica* A **82** 221
[21] Bedeaux D and Vlieger J 1983 *Thin Solid Films* **102** 265
[22] Wilson K G 1971 *Phys. Rev.* B **4** 3175
Wilson K G 1971 *Phys. Rev.* B **4** 3184
[23] Yuge Y and Murase C J 1978 *J. Phys. A: Math. Gen.* **11** L83
[24] Reynolds P J, Klein W and Stanley H E 1977 *J. Phys. C: Solid State Phys.* **10** L167
[25] Kadanoff L P 1975 *Phys. Rev. Lett.* **34** 1005
[26] Abeles F 1950 *Ann. Phys., Paris* **5** 777